Talanta Open 5 (2022) 100111

Contents lists available at ScienceDirect

Talanta Open

journal homepage: www.sciencedirect.com/journal/talanta-open

Development of mini column experiments (MCE) by coupling microliter flow HPLC with ICP-MS for the analysis of metal retention under conditions close to nature

Ralf Kautenburger *, Kristina Brix, Sandra Baur, Jonas Michael Sander

Elementanalytik – WASTe, Anorganische Chemie, Universität des Saarlandes, Campus C 41, 66123 Saarbrücken, Germany

ARTICLE INFO

Keywords:
Mini-column experiments
Microliter flow
HPLC-ICP-MS coupling
Europium
Opalinus clay

ABSTRACT

The development and implementation of mini column experiments (MCE) can be of great importance to improve existing analytical methods such as highly standardised but unrealistic batch laboratory experiments or lengthy long-term diffusion experiments to study metal sorption/desorption properties. One envisaged application would be to test the retention of repository-relevant metals in claystone, which is a promising candidate for the host rock of a final repository site for high-level radioactive waste (HLW). The used MCE setup is derived from classical high performance liquid chromatography (HPLC). On this basis, coupling of MCE to ICP-MS (inductively coupled plasma mass spectrometry) detection was realised. This online separation enables the dynamic monitoring of metal sorption and desorption experiments on clay minerals (kaolinite), natural clay (Opalinus Clay) and mixtures with quartz sand in background solutions close to nature, and without the common use of metal complexing ligands, other reaction partners or buffers for the analysed metal ions. The optimised method allows the analysis of the retention of various contaminants in real groundwater solutions and compact clay samples in a reasonable amount of time and a small amount of sample. In addition, the coupling to the unspecific mass detector of ICP-MS enables the study of different radionuclides and homologues rather than the limited UV detection of a common HPLC.

1. Introduction

For the reliable long-term safety analysis of a repository for high-level radioactive waste in deep geological formations, knowledge of the interaction processes resulting in potential mobilisation or retention of radionuclides is essential. Clay rock is considered as a natural host formation as well as in the form of bentonites as backfill or sealing material for nuclear repositories in deep geological formations. In addition to the naturally occurring host rock, the geotechnical barrier also plays an important role for the mobility or retardation of radionuclides. The sorption and retention properties of the host rock are of particular interest in this context since these are decisive for the safe disposal of the radioactive and toxic repository inventory [1–3].

By performing classical diffusion experiments, the migration of pollutants along a concentration gradient of compact rock material such as clay drill cores can be investigated. This can be done targeted and yet very close to nature on a laboratory scale or on a larger scale in rock laboratories in-situ. However, diffusion in clay stone, especially of higher valent metal ions is a slow process [4–7]. Therefore, such experiments with running times up to several years are long-term experiments, but they provide important insights into the diffusion behaviour and direct access to parameters such as the diffusion coefficient of a metal in the host rock of the potential repository. At the other end of the experimental time scale are the so-called batch experiments [7–10]. Batch experiments are test series in which a set of many individual samples is investigated under precisely defined conditions, which enables the reliable determination of measurement data such as adsorption or desorption isotherms and partition coefficients (K_d or R_d values) as a function of the test parameters used [11,12]. However, with a high water or matrix content and a low solid content, they correspond more to the scenario of considerable water influx into an existing repository and are thus in conceptual contrast to the diffusion experiments on compact rock cores. In addition, ground and homogenised powdered clay is used for the execution. In order to be able to determine K_d values under more realistic conditions, classical geological column experiments are usually carried out [10,13,14], in which comparatively large

* Corresponding author.
E-mail address: r.kautenburger@mx.uni-saarland.de (R. Kautenburger).

https://doi.org/10.1016/j.talo.2022.100111
Received 23 December 2021; Received in revised form 23 March 2022; Accepted 24 March 2022
Available online 26 March 2022

columns with internal diameters in the range of centimetres and lengths of up to several decimetres are used [15–18]. A main disadvantage of classical geological column experiments is the time required for sorption and desorption experiments as well as the large space requirement due to the size of the column but also for the peripheral equipment and the large amount of sample material required to fill the large columns.

Miniaturized column experiments have existed predominantly only in the application of micro monolithic columns and predominantly only for couplings with high-pressure gas chromatography (GC), e.g., for separation of gas mixtures [19] or fused-silica capillaries when coupling capillary electrophoresis (CE) with ICP-MS for separation of e.g., Gd species or nanoparticles by Taylor dispersion analysis (TDA) [20]. However, such methods or columns cannot be used to perform sorption experiments of metal ions with natural clay materials, as is the case with classical geological column experiments or the mini-column experiments described here.

In a past study miniaturized clay column experiments for sorption studies of metal ions with clay minerals were developed as an intermediate between batch and diffusion methods in terms of both their setup and experimental duration [11]. This first stage of development was generally comparable to classical column experiments, but they eliminate one of the major disadvantages of classical column methods by requiring significantly less time and sample material per experiment. While in the diffusion experiments only diffusion processes determine the migration of the metal cations under investigation, in the batch experiments, single diffusion is negligible due to the small particle size of the homogenised clay. In the miniaturized clay columns the weak and anyway slow diffusion processes was completely overlaid by the advective flow in the column [6]. They allowed the investigation of sorption, desorption, precipitation, and remobilization effects on the retention of the relevant metal cations on the clay in a dynamic way. As an example, this was necessary for the analysis of trivalent actinides where Eu(III) is commonly used as a homologue. The experimental parameters could be easily varied, due to the derivation from classical HPLC [15]. In this previous work the columns were packed with pure clay as stationary phase, which resulted in extremely low fluxes in the lower microliter per minute range. As a result, individual experiments took many days to complete [21]. Shortening the duration of such an experimental run to 10–20 min per injection would significantly increase the practicability of mini-column experiments. In addition, detection in the first stage was still carried out exclusively by means of UV–Vis detection via a diode array detector and was therefore completely unsuitable for metals and analytes in the trace range [15]. Therefore, the optimisation of the mini-column experiments is required to reliably observe the elution of the injected metals. Coupling with an element-sensitive detector such as inductively coupled plasma mass spectrometry (ICP-MS) can make very significant advances in this regard.

The use of coupling methods such as HPLC-ICP-OES or HPLC-ICP-MS for the separation of inorganic ions has been applied for a long time, but classical exchange columns as well as complexation ligands are used to separate the metal species [22–26]. However, for a realistic observation of metal retention under repository-relevant conditions, no metal-complexing ligands, reaction partners or buffers as well as synthetic stationary phases with functional groups may be used. These unnatural changes in the experimental conditions would make a realistic picture of metal retention in natural rock formations and real groundwaters impossible. Therefore, this paper presents a novel experimental design of mini-column experiments (MCE) in the microliter flow range using realistic background solutions and various natural column filling materials. Customary high performance liquid chromatography (HPLC) has been modified and coupled to inductively coupled plasma mass spectrometry (ICP-MS) as detector to make further advances in the development of analytical methods for the long-term safety analysis. The presented MCE-ICP-MS method enables dynamic sorption and desorption experiments of Eu(III) as a chemical analogue of trivalent actinides in compacted quartz sand as well as in claystone under near natural conditions. In comparison to classical diffusion or classical column methods, which require several months, MCE-ICP-MS results are obtained within a few minutes or hours depending on the used analyte and experimental setup. Additionally, the methodology can be applied to many other related geochemical problems as the solid phase can be varied easily. Furthermore, the choice of trivalent europium as analyte demonstrates that the optimised MCE-ICP-MS method even works for metals with a very high sorption capacity.

2. Experimental

2.1. Materials and methods

2.1.1. Chemicals and standards

All standards and chemicals were of p.a. quality or better (e.g. emsure or suprapure) and were obtained from Merck (Darmstadt, Germany). Ultrapure water (18.2 MΩ cm) (deionisation system PURELAB Chorus 1 (VWS (UK) Ltd., trading as ELGA LabWater, UK) was used to prepare all solutions. The single element standards CertiPUR® of europium (Eu(III)) (10 g L^{-1}), scandium (Sc(III)) and holmium (Ho(III)) (1 g L^{-1} respectively) were also obtained from Merck. Sc(III) and Ho(III) were diluted 1 : 100 in ultrapure water and used as spike and internal standard solution for all experiments. For adjusting the pH value, perchloric acid (70%, suprapure) and NaOH (emsure analytical grade by Merck (Darmstadt, Germany) were applied. Argon 5.0 (99.999%, ALPHAGAZ™ 1 ARGON, Air Liquide Deutschland GmbH, Düsseldorf, Germany) was used as plasma gas for ICP-MS measurements. For background solution ultrapure water was used. For the MCE Eu(III) as trivalent metal cation is used as model analyte, and 1-bromopropane, sodium bromide and iodide (Merck, CertiPUR®), were used as inert marker testing the experimental set up of MCE.

2.1.2. Opalinus Clay, kaolinite and quartz sand

Natural Opalinus Clay (OPA) was used, which was provided in the form of several drill cores by the Federal Institute for Geosciences and Natural Resources (BGR) and originates from the underground laboratory at Mont Terri in Switzerland (OPA BLT-14). The core sample was stored in containers with 0.5 bar Ar overpressure. The aerobe homogenate of the clay was obtained by milling the clay to a fine-grained powder with a particle size smaller than 500 μm [9,27]. The undestroyed OPA represents a well characterized clay [28] with a cation exchange capacity (CEC) ranging from 9 to 12 meq 100 g^{-1}, the porosity of the sample was 10.8% [29]. In addition, kaolinite KGa-1b (Georgia, USA), sold by the Clay Minerals Society (Chantilly, USA), and quartz sand were also used as stationary phases in the column. Due to the known strong swelling behaviour of OPA it is not possible to fill 100% OPA into the mini-column. The OPA was mixed with parts of quartz sand. Contrary to the OPA, kaolinite can be used in the HPLC column as reference mineral without relevant swelling behaviour. The quartz sand (purified sea sand) is commercially available from Merck KGaA (Darmstadt, Germany).

2.1.3. Determining of the dead time

To determine the dead time t_0 of a classical chromatographic column, the time from injection to elution of a detectable inert marker in the chromatographic system with column included is measured. Only when the marker substance has been transported at the flow rate of the mobile phase is the determination of the dead time t_0 reliable. If the inert marker is retarded at one or more points within the system, i.e. does not react inertly, the dead time is erroneously increased. If the marker substance is excluded from the stationary phase, this again leads to an erroneous reduction of the dead time [30]. Due to the absence of an ideal inert marker in our experiments with natural column filling materials and background solutions, we determined the dead time t_0 and porosity ε of the columns used in a different, indirect way. The investigated

column is preconditioned by a constant flow of 40 µL min^{-1} with an eluent mixed with uncharged 1-bromopropane (10 µL 1-bromopropane in 500 mL ultrapure water), and the signal intensity of ^{79}Br is recorded by ICP-MS as demonstrated in section 3.2.5.

2.1.4. Porosity of the column packing

Using the correctly determined dead time t_0, the total porosity ε of the column packing material can be calculated [30]. The total porosity ε is the fraction of the total column volume occupied by the mobile phase:

$$\varepsilon = \frac{V_{column} - V_{filling}}{V_{column}} \quad (1)$$

For the experimental determination of ε the following formula is used where d is the inner diameter of the column:

$$\varepsilon = \frac{4 \cdot V \cdot t_0}{d_c^2 \cdot \pi \cdot L_c} \quad (2)$$

Common values for the porosity of chemically bound phases (e.g. C_{18} phases) used as stationary phase in a common chromatographic system are in the range between 0.6 and 0.8 (ideally approx. 0.65). Values above 1 show that the substance used for the determination did not migrate at the speed of the mobile phase resulting in delayed elution due to the mobile phase retaining the substance. If the values are below 0.5, the substance was excluded from the pores of the column stationary phase and migrated faster than the true dead time. In the last two cases, the substance is considered unsuitable for determining the dead time. If pure silica gel or non-porous particles are used as the stationary phase, the limits for an occurring retention of the inert marker are 0.75 and for exclusion are 0.4 [30]. The modified determination of the total porosity ε for the used clay/quartz columns is shown in chapter 3.2.5.

2.2. Instrumentation

2.2.1. Mini-column experiments (MCE) setup

In this study an Agilent 1100/1200 HPLC system (Agilent, Waldbronn, Germany) was used for the MCE (Table 1). The HPLC system consists of a HPLC pump with constant flow rates between 0.5 µL and 2 mL per minute between 1 and 400 bar. The samples are injected by an autosampler with a sample volume between 0.1 and 100 µL. Larger volumes can be added continuously as a second eluent solution. The column (C-270, Upchurch Scientific, enlarged to 20 mm x 3.5 mm ID) can be filled with clay (OPA or kaolinite) as stationary phase (sorbent) or using a variable mixture with purified quartz sand (total weight of about 250–300 mg per column). The temperature of the column can be controlled exactly between 15 and 80 °C in a column compartment. After separation in the column the different sample species can be detected via a diode array detector (DAD) or additionally by coupling with ICP-MS to detect the UV/Vis-inactive species.

As mobile phase (eluent) different combinations of solutions can be mixed by a binary capillary HPLC pump. In our experiments usually ultrapure water (Milli-Q) as background solution is used as mobile phase. Iodide or bromide was used as mobility (retention time) reference to check the repeatability of each experiment by adding 0.1 mM NaI or NaBr into all samples to correct the differences of the retention time in different experiments as well as in the different clay columns used.

Table 1
Components and software of the HPLC apparatus used.

Agilent Series 1100	Agilent Series 1200
Solvent cabinet	Analytical fraction collector G1364C
Vacuum degasser G1379A	Fluorescence detector G1321B
Capillary pump G1376A	
Binary pump G1312A	
Automatic sampler G1313A	
Column thermostat G1316A	
UV Vis diode array detector G1315B	

Software used: ChemStation for LC 3D Systems Rev.B.02 0.01-SR2 [260] 58.

2.2.2. Mass spectrometry with inductively coupled plasma (ICP-MS)

An Agilent 7500cx ICP-MS (Agilent Technologies, Santa Clara, USA) with ORS collision cell was used for coupling and the isotope measurements of the used analytes. Detailed analytical conditions are given in Table 2.

2.2.3. MCE coupled to ICP-MS

For the coupling of HPLC and ICP-MS (see Fig. S1 in the Supplemental information, SI) the setup has been modified to obtain better sensitivity and faster response. This has been done by both minimising the dead volume of the system and exchanging the standard nebulizer and the spray chamber of the ICP-MS system. The outlet of the HPLC column can be directly connected to the ICP-MS nebulizer inlet thus bypassing the HPLC detectors (such as the diode array). The detailed optimisation of the MCE-ICP-MS can be found in the results and discussion section.

3. Results and discussion

3.1. Characterization of the Opalinus Clay

The used Opalinus Clay (OPA, BLT-14) [31] provided by BGR (Federal Institute for Geosciences and Natural Resources) and homogenised by KIT (Karlsruhe Institute of Technology) was first characterized by powder diffraction (XRD). The percentage OPA phase fractions obtained are shown in Table 3 in comparison with the averaged results of the Swiss NAGRA drilling at the Mont Terri underground rock laboratory in Switzerland [28].

In addition to the two single clay minerals kaolinite and illite, BLT-14 also contains quartz, calcite, and small amounts of pyrite. Moreover, small amounts of other, unspecified, secondary phases are present. If the current BLT-14 clay is compared with the earlier model clay BHE-24/1, all phase fractions within the measurement uncertainty are consistent except for the significantly higher calcite content of 18 ± 3% in the new model clay BLT-14 compared to 13 ± 1% for BHE-24/1 [9].

A sample of the BLT-14 clay was examined with a scanning electron microscope (JEOL JSM-7000 F, Tokyo, Japan). An image that shows the heterogeneity of the BLT-14 batch particularly well is shown in Fig. 1A. The layered structure of the clay minerals contained can be seen at

Table 2
Operating parameters of the Agilent 7500cx ICP-MS for the measurement routine during coupling with HPLC.

Parameter	Value
ICP-MS	Agilent 7500cx
RF-power	1550 W
Plasma/auxiliary/ nebulizer gas	15.0/1.05/1.0 L min^{-1}
Sampler / skimmer diameter orifice	Nickel 1.0/0.4 mm
Dwell times / Repetition	100 ms per mass/3 times
Nebulizer	Glass Expansion MicroMist
Liquid flow	0.42 mL min^{-1}
Spray chamber temperature	2 °C
Acquisition mode	Time resolved analysis
HPLC system	Agilent 1100/1200
Column	Home made 20 mm x 3.5 mm ID; modified from C-270, Upchurch Scientific, Oak harbour, USA
Mobile phases	Ultrapure water
Flow rate	1–40 µL min^{-1}
Injection volume	1–5 µL
Samples	
Sc, I, Cs, Eu, Ho, U (ICP standards)	certipur® (Merck), diluted in ultrapure water
Analysed isotopes	^{45}Sc, ^{79}Br, ^{127}I, ^{133}Cs, ^{153}Eu, ^{165}Ho, ^{238}U
Quantification	ICP-MS FullQuant mode

Table 3
Phase fractions (in%) after structure refinement [32] of the powder diffraction diagrams of Opalinus Clay samples from batches BLT-14 ($n = 3$) in comparison with Nagra's mean values for drillings in Mont Terri ($n = 8$; exclusive sandy-limestone facies).

Phase	BLT-14	Mont Terri [28]
Quartz	20 ± 4	14 ± 4
Calcite	18 ± 3	13 ± 8
Kaolinite Serpentine	37 ± 2	nd[1]
Kaolinite		22 ± 2
Illite	24 ± 2	23 ± 2
Illite/semectite	nd[1]	11 ± 2
Pyrite	0.9 ± 0.6	1.1 ± 0.5
Feldspar	< 4	1.0 ± 1.6
Chlorite	< 5	10 ± 2
Siderite	nd	3.0 ± 1.8
Dolomite/Ankerite	nd	< 1
Albite	nd	1 ± 1

[1] nd: not determined.

higher magnification of another position in Fig. 1B.

3.2. Mini-column experiments (MCE)

3.2.1. Filling the columns for MCE

Two different methods were tested for filling the columns. Firstly, wet filling with a clay slurry (suspension or slurry) and secondly, dry filling. Filling the column with a clay suspension proved to be difficult due to the small inner diameter of the columns (3.5 mm). Attempts to either apply negative pressure at the column outlet or to fill the suspension into the column by means of pressure, e.g. using a piston syringe with or without a cannula attached, proved to be impractical. Filling the column using a funnel that could be screwed onto the column inlet was not practical either. The thixotropy described in the literature for tone-in-water suspensions, i.e. the decrease in viscosity of a non-Newtonian fluid under the influence of shear forces [33,34] could not be exploited either. In addition, the exact determination of the amount of clay in the column during wet packing is inaccurate and further complicated by the swelling of the swellable clay minerals as stationary phase and the associated change in volume. For these reasons, packing the columns with dry packing material without prior moistening or swelling of the packing material in a solvent was preferred. The procedure is based on the description of J. Klawiter et al. [30,35]. It should be mentioned that particles with a diameter smaller than 20 μm cannot be packed dry because of aggregation resulting in lumps [30]. However, such aggregation is not to be expected in our case due to the polydispersity of the particle diameter, and the irregular shape of the clay particles. Furthermore, in the case of the clay-quartz sand mixtures the addition of the quartz sand additionally prevents the formation of agglomerates.

Fig. 2 shows the clay before use in an MCE (loose pourable clay particles), and clay compacted by the mobile phase during the experiment, which was recovered from the column after an MCE. Also shown is an HPLC column (stainless steel guard column holder C-270, Upchurch Scientific, Oak Harbour, USA, drilled to 3.5 mm I.D.) disassembled before filling.

When trying to use pure OPA as column packing for MCE, the columns are blocked very soon due to the swelling of the clay by contact with the eluent. The pressure required to continue pumping the mobile phase through the column rises rapidly from a few bar backpressures at the beginning of the experiment to over 200 bar before the column is completely blocked. This process makes any further use of the column impossible. Columns in which the powdered OPA is further diluted with quartz sand before packing can be saturated with eluent at low flow rates (< 10 μL min^{-1}) after packing and purged from air. Quartz sand is a suitable choice since it is already present in the natural OPA in amounts of about 20% (see Table 3). However, the initial wetting of the column packing material with the background solution is still very sensitive to pressure fluctuations. Therefore, the HPLC flow must be increased stepwise (about 1 μL min^{-1}) to reach the usual flow rate of about 20–40 μL min^{-1} for the beginning of MCE. For saturation at low concentrations of the analyte in the ppb or ppm range, more than 40 h are necessary to achieve breakthrough on pure OPA columns at the respective concentration level (result of own previous experiments). This is another reason for packing clay columns diluted with quartz sand. The dilution of OPA with quartz sand was prepared using an intermediate dilution as follows: 1.00 g OPA is mixed with 9.00 g quartz sand in a plastic container with a screw cap, both by repeated shaking and by stirring with a spatula. Exactly 1.00 g of this intermediate dilution is taken and mixed again with 9.00 g of quartz sand in a new container. In this way, a column filling with an OPA content of 1 wt.% is obtained for use in MCE.

3.2.2. Setup and optimization of the HPLC(MCE)-ICP-MS coupling

When establishing the coupling between HPLC and ICP-MS for MCE, both instruments were initially used in their standard configuration (as shown in Fig. 3A) and the outlet of the DAD of the HPLC was connected to the inlet of the peristaltic pump tube of the ICP-MS via a PEEK Tee (P-727, Upchurch Scientific, Oak Harbour, USA) using a standard HPLC capillary made of PEEK plastic (inner diameter 0.17 mm). To achieve the eluent flow of about 0.4 mL min^{-1} which is necessary to generate a stable aerosol flow in the default nebulizer of the ICP-MS, a make-up liquid was added via the T-piece. For this purpose, nitric acid (3%) was taken from a storage vessel with an external peristaltic pump and added to the flow to the nebulizer of the ICP-MS as shown in Fig. 3A).

Nevertheless, a memory effect or carry-over from one experiment to

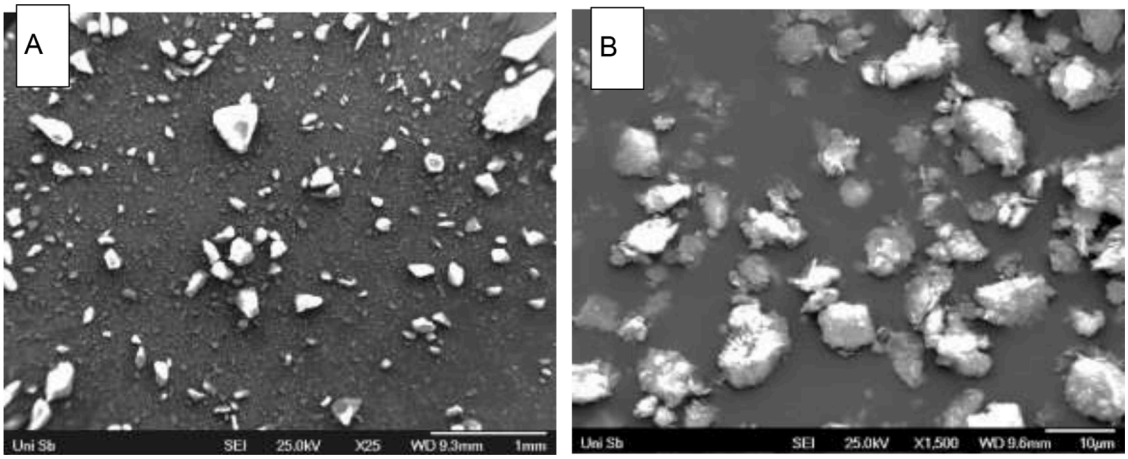

Fig. 1. Scanning electron microscope image of a sample of the BLT-14 Opalinus Clay at 25x (A) and 1500x (B) magnification.

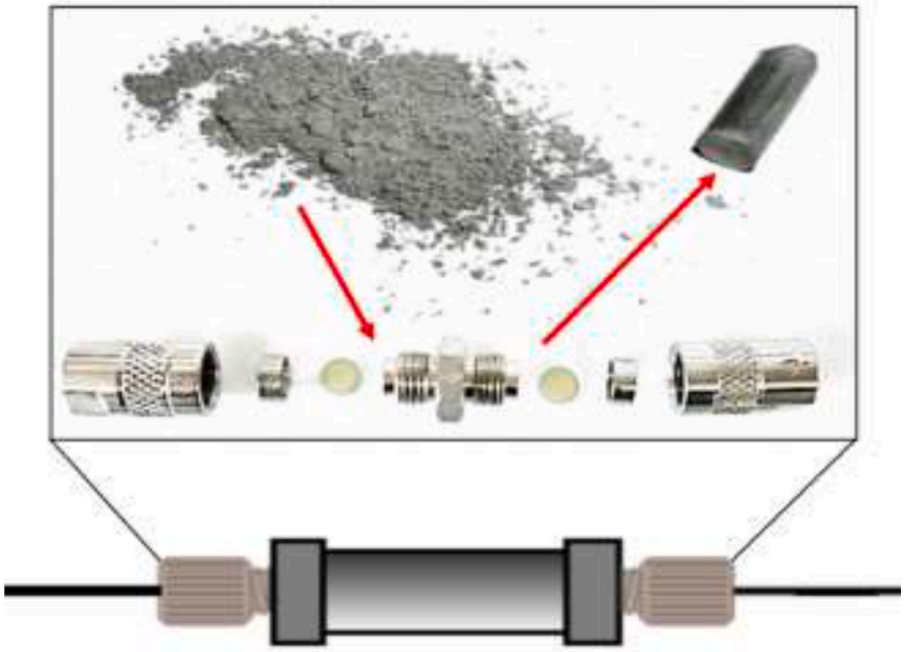

Fig. 2. Mini-column setup and clay before (left hand side) and after (right hand side) a typical MCE experiment. Shown is pure Opalinus Clay (OPA) as powder before filling and compacted by swelling and eluent flow after use as column packing. Additionally, there is shown a column disassembled into individual parts.

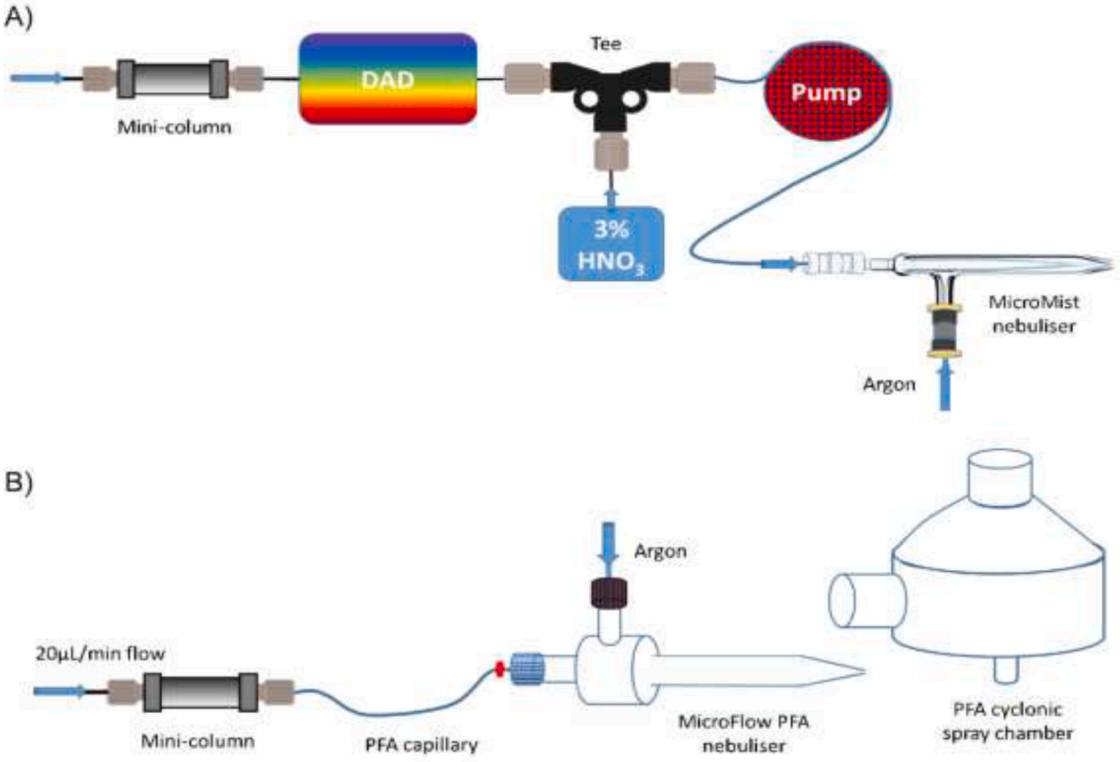

Fig. 3. First setup of the MCE coupling to ICP-MS (A) and optimised setup of the MCE-ICP-MS coupling (B).

the next was observed with this initial set-up, even though nitric acid was added to prevent wall adsorption. The Glass Expansion MicroMist glass nebulizer, used as standard in the Agilent 7500cx, and the Scott spray chamber, also made of standard borosilicate glass, could be identified as the cause of the observed memory effects. To avoid the interferences that occurred, the standard configuration (Scott spray chamber and MicroMist nebulizer) was replaced by a PFA (perfluoroalkoxy polymer) MicroFlow nebulizer (flow: 20–50 µL min^{-1}), and a 20 mL cyclonic spray chamber made of PFA (both from Elemental Scientific, Omaha, USA) as shown in Fig. 3B).

Compared to the Scott spray chamber, the cyclonic spray chamber also offers the advantage of a low internal surface area, which is better flushed due to the stronger swirling of the aerosol inside the chamber [36]. Also, the addition of the make-up flow via the T-joint can be

omitted now. Therefore, the sensitivity is increased because the eluate is not further diluted before the ICP-MS measurements. Furthermore, the column used in each case was directly connected to the nebulizer inlet without a bypass via the DAD module of the HPLC located between the column and ICP-MS. A PFA capillary (flow range of 20–50 µL min^{-1} with self-priming operation of the nebulizer with 1.0 L min^{-1} argon) was used for this purpose (inner diameter 0.15 mm). This eliminates the widening of the sample zone due to the flow through the Z-cell in the diode array. In addition, the peristaltic pump tube to the nebulizer is eliminated to prevent possible memory effects. The good inertness of the entire HPLC (MCE)-ICP-MS system can be demonstrated by means of injections of trivalent Eu ions (2 mM Eu(III)perchlorate solution) using a HPLC PEEK Union (P-742, Upchurch Scientific, Oak Harbour, USA) without dead volume (Union ZDV) instead of the column as seen in Fig. 4.

3.2.3. *Validation of the analytical system*

In many analytical investigation methods, the influence of any memory effects must be minimised and ideally completely prevented so that falsification of the analytical results obtained can be avoided. In the apparatus used for MCE, such falsification can occur due to adsorption on the walls of liquid-carrying pump components, capillaries, inner column wall, transfer line from HPLC to ICP-MS, and nebulizer chamber wall. For the column filling material, it must be ensured that the quartz sand which is used for diluting the OPA does not serve as adsorbent for the metals studied. In addition, the influence of quartz sand-OPA mixtures on the adsorption capacity should be known and corrected to draw conclusions about the sorption properties of pure OPA.

To test the memory effect of the HPLC-ICP-MS system used for MCE, a blank without dead volume (Union ZDV) was initially used instead of the column. In the case of injection-based MCE, the inertness was checked by means of injections both via the Union ZDV connector and via a column filled only with pure quartz sand. Fig. 4 shows the measurement and evaluation of a tenfold injection of 5 µL each of a 2 mM europium perchlorate solution via the Union ZDV connector. The ^{153}Eu signal shows narrow signals with very slight tailing and Eu(III) peaks are baseline-separated after each injection.

The first two Eu(III) injections show a slight underestimation compared to the heights of the remaining eight peaks due to the adsorption of Eu(III) in the HPLC system. The peak heights of injections 3 to 10 shall be considered equal within the measurement uncertainty of about 6.2% (see Table S1 in the SI). Adsorption in the system can also be identified from the peak areas based on the sub-findings of the first two peak areas. The remaining peak areas are within the range of the error bars (SD = 5.6%; in relation to the areas of injections 3 to 10).

However, a continuous increase in peak areas would also be compatible with the data shown. Although, the differences of all peak areas are within the range of the error bars. The same peak shape and the rapid return to the baseline are also shown here (Fig. 4). With the same amount of metal injected, the fluctuations in peak height are greater than the fluctuations in peak area, so the peak area (Fig. 4B) is used here for quantification.

If the mean value A_{Peak} of the peak areas is calculated from the injections i= 3 to i= 10 (see Table S1 in the SI), the result is

$$\overline{A}_{\mathbf{Peaks}3-10} = \frac{\sum_{i=3}^{10} \boldsymbol{A}_{\boldsymbol{Peak}}\ (\boldsymbol{i})}{\boldsymbol{i}_{\boldsymbol{total}}} = \frac{8,128{\cdot}10^{6}\ \mathbf{counts{\cdot}s}}{8} = 1,016{\cdot}10^{6}\ \mathbf{counts{\cdot}s} \quad (1)$$

with a percentage standard deviation of 5.6%.

The calculated average peak area corresponds to an injected amount of Eu(III) of

$$n_{inj}\ (Eu(III) = V_{inj} \cdot c_{inj} = 5\ \mu\mathbf{L} \cdot 2\frac{\mathbf{mmol}}{\mathbf{L}} = 10\ \mathbf{nmol} \quad (2)$$

per injection.

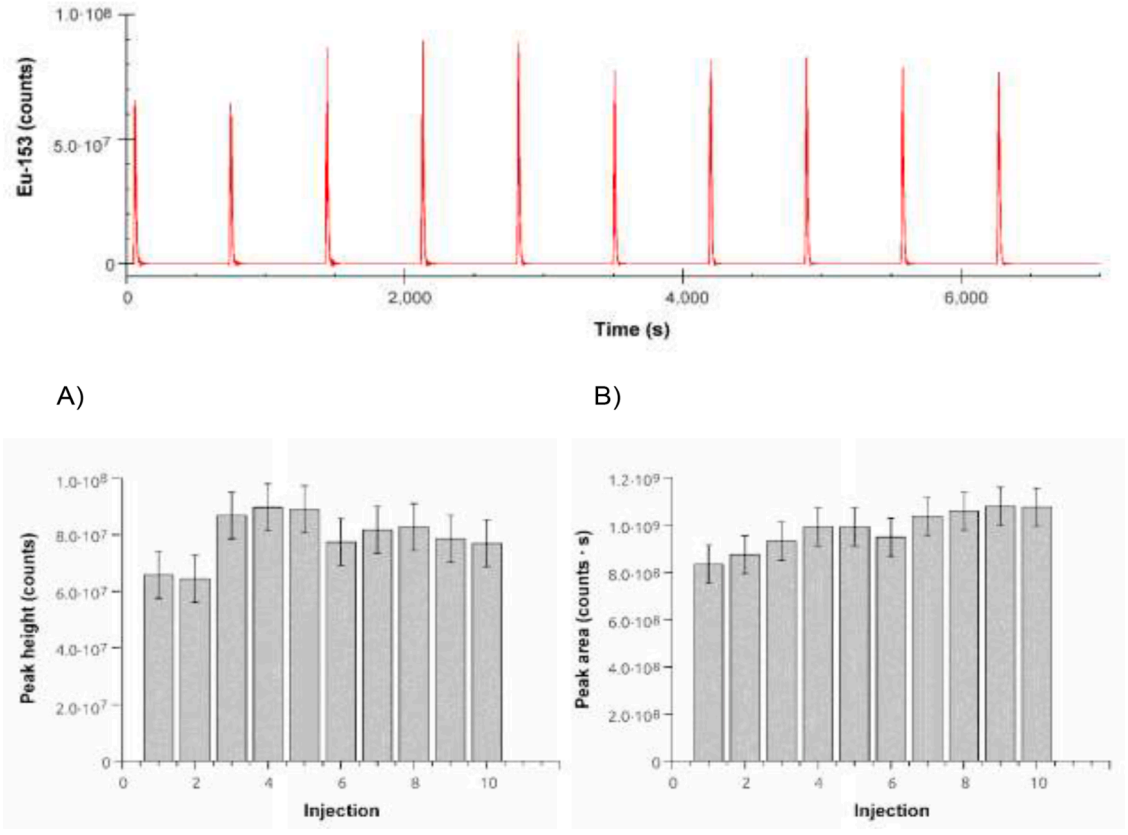

Fig. 4. Measurement and evaluation of a tenfold injection of 5 µl each of a 2 mM europium perchlorate solution via Union ZDV as part of an MCE (eluent: 40 µL min^{-1} Milli-Q ultrapure water); peak height A) and peak area B) of the above shown peaks.

The respective difference between the mean value of the peak areas of the injections of three to ten $\bar{A}_{Peak3-10}$ and the first two injections with a clear underestimation amounts to 181,256,418 and 139,897,063 counts · s, respectively and corresponds to an under-record of Eu(III) of

$$n_{memory,1}\ (Eu) \approx 1.784 nmolor(Eu) \approx 1.377 nmol$$

or added up over both injections

$$\sum_{i=1}^{2} \boldsymbol{n_{memory,1}}\ (\boldsymbol{Eu}) = 3.161\ \mathbf{nmol}. \quad (3)$$

If all peaks with a numerical underestimation compared to the above mean value (i= 1 to i= 6) are added up, a quantity of Eu(III) sorbed in the system of 5.069 nmol is obtained [10]. Thus the series of experiments show, that at the beginning of a measurement, a significant amount of Eu(III) remains in the system. This fact applies to the first measurement series of the day as well as to the first measurement series with Eu(III). The "missing" europium is presumably adsorbed on the inner surfaces of the eluent carrying components. The extent of the memory effect is, with about 16% in relation to the first two injections (3.161 nmol/20 nmol · 100%) or about 3% in relation to all ten injections (3.161 nmol/100 nmol · 100%), and a sum of about 5% of the first six in relation to all ten injections (5.069 nmol/100 nmol · 100%). Since only the first injections of a measurement day led to a serious deficit of Eu(III), all further experiments are performed with injections up to saturation of the HPLC and ICP-MS system via the Union ZDV before the mini-column is installed in the previously saturated system. To achieve the saturation, three injections with a higher Eu(III) concentration than used during the measurement series were used.

For the subsequent tests of the retention behaviour of Eu(III) on OPA, the clay must be diluted with additional quartz sand before being filled into the mini-columns due to its high swelling and sorption capacity. For this reason, the sorption capacity of the pure quartz sand for Eu(III) was determined by repeated injections of the metals through a mini-column filled with quartz sand followed by calibration experiments with a quartz/clay column. Therefore, a wider calibration range based on injections of several concentration values are presented in the following section.

3.2.4. External calibration for Eu(III) recovery in MCE

For the quantitative evaluation of MCE, an external calibration of the ICP-MS with HPLC coupling must be performed. Afterwards, the calibration data can be used to determine the parameters that need to be converted into concentration data for the signals (peak areas) of Eu(III) detected during the MCE with clay columns. Initially, the europium signals and calibration curves via the Union ZDV as well as for a column with 293 mg quartz sand are carried out (see Fig. S2 and Fig. S3 in the SI). After integration, the graphs for the calibration curves are generated from the peak areas, respectively. The peak areas of the quartz sand column are larger compared to the Union ZDV, since the injected sample volume is affected by the column filling divergencies. The time offset between the two measurement signals is due to the different dead volume of the Union ZDV connector or quartz sand column. In addition, ultrapure water was injected once (quartz sand column) or twice (Union) at the beginning of the data recording.

Calibration is carried out using a clay column previously saturated with Eu(III) until complete breakthrough (1 wt.% OPA). The calibration curve is shown in Fig. 5.

The peaks of the injections via the filled column are significantly broader than the injections via the Union ZDV. In both cases the signals show a tailing, which is even more pronounced in the case of the 1 wt.% clay column than for a column filled with only quartz sand. On the one hand the column filling itself and on the other hand also the widening of the flow path to the inner diameter of the column contribute significantly to the peak broadening. Additionally, a further peak broadening is expected with the change from the relatively homogeneous quartz sand as column filling to the clay columns diluted with quartz sand.

In Fig. 6 normalized peaks after injection via the Union ZDV and the column filled with quartz or quartz sand-clay mixture are shown. The filling with the quartz sand-clay mixture indeed leads to a significant broadening of the peak compared to the pure quartz sand filling. Thus, even the small percentage of only 1 wt.% OPA in the column has a significant influence on the peak form. Despite all peak-widening influences and the occurrence of tailing, the underlying Gaussian shape of the peaks is still clearly recognisable in Fig. 6.

Table 4 shows a comparison of the obtained calibration functions and the corresponding figures of merit. The gradient and thus the sensitivity of the measurements are comparable for the different columns: While the sensitivity increases significantly from the Union ZDV to the quartz column, it decreases slightly towards the clay column. This fact contradicts partly the expectations: A high sensitivity is estimated for the Union ZDV, where the slightest influence on injected sample arises and no sorption occurs at the (non-existent) column packing. A decrease in sensitivity is expected from Union ZDV piece to pure quartz sand filling and from the pure quartz sand filling to the clay column filling. The variation in ICP-MS instrument sensitivity from day to day is since the calibration functions were recorded on different days. Overall, the standard deviations of the determined slopes (σ_a) of the Union ZDV (0.82%) and the quartz column (0.45%) are comparable. However, the standard deviation of the slope of the OPA column is higher by a factor of around 10 (6.8%). Hence, the individual measuring points for each concentration of the calibration scatter more strongly. Resulting in a

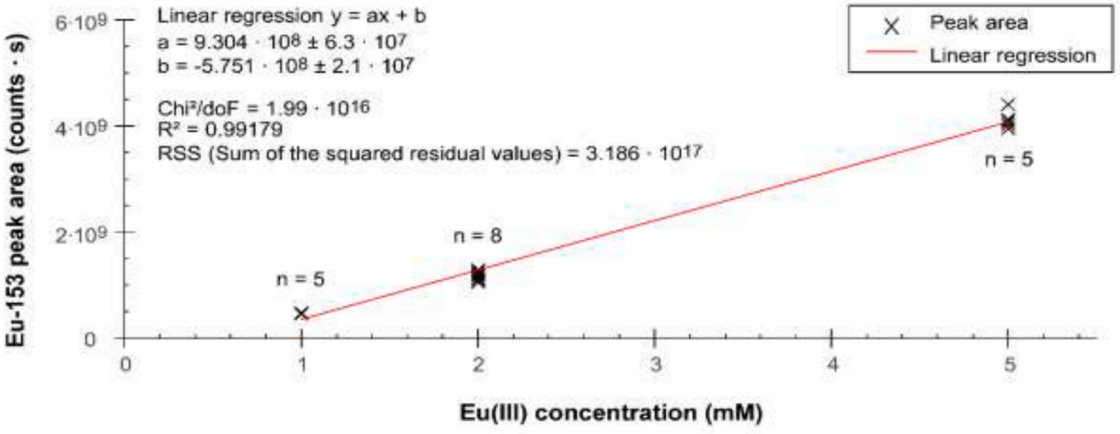

Fig. 5. Calibration graph of peak areas as a function of injected Eu(III) concentration (5 µL injection of 1, 2 and 5 mM Eu(III) at a flow of 40 µL min^{-1}, respectively) and linear regression for a 1 wt.% OPA clay column. In this case the calibration was done from the highest to the lowest concentration.

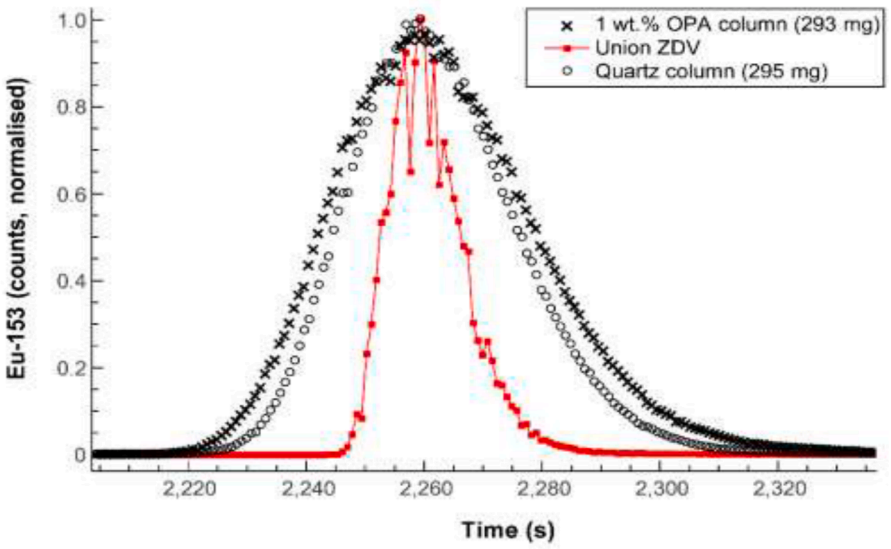

Fig. 6. Representative comparison of the normalised measurement signals after injection across the different columns or column fillings used (5 µL injection of 2 mM Eu(III) at a flow rate of 40 µL min^{-1}, respectively). The data points were shifted along the abscissa so that the peak maxima are congruent for better comparison.

Table 4
Comparison of the calibration parameters and figures of merit according to the linear function $y = a \cdot x + b$. a: slope (10^8 counts · s · $(mM)^{-1}$), σ_a: standard deviation of slope (10^8 counts · s · $(mM)^{-1}$), b: ordinate intersection point (10^8 counts · s), σ_b: standard deviation of the ordinate intersection point (10^8 counts · s), R^2: Pearson-corellation coefficient.

Column	a	σ_a	b	σ_b	R^2
Union ZDV	4.65	0.038	−1.80	0.01	0.9989
100 wt.% quartz	11.50	0.052	-3.03	0.30	0.9996
1 wt.% OPA	9.30	0.630	−5.75	0.21	0.9918

higher error of the slope of the calibration line of the clay column. The increased scattering is due to the escalating complexity of the column filling: Starting with a Union ZDV without appreciable influence on the injected sample zone over a quartz sand filling to a filling of quartz sand and natural OPA (consisting of a multi mineral mixture).

Negative ordinate intersections result for all three column types, with the negative distance from origin increasing from the Union ZDV above the quartz sand column towards the clay column. With identical gradient or sensitivity of the regression line, a parallel shift of the line along the abscissa (concentration axis) would result in an increase of the limit of detection (LOD) and consequently the limit of quantification (LOQ). A rough estimate as shown in the SI gives an LOD of 1.8 µM and an LOQ of 3.5 µM for the Eu(III) at the used conditions (SI, page S3). Pearson correlation coefficient (R^2) allows a statement to be made about the linearity of the correlation between abscissa and ordinate values of the calibration curves, whereby the R^2 values in all three cases are close to 1.0 overall. While the R^2 values of the Union ZDV and the quartz column do not differ significantly, the correlation coefficient for the calibration with the clay column is slightly smaller, which could be explained by the more inhomogeneous column filling.

3.2.5. Dead time and porosity of the column types

The dead time of a chromatographic system can be determined by injecting an inert substance via the used column and time measurement until its detection. Since other methods for the reliable determination of the dead time, such as the use of radioactive substances, have been ruled out for various reasons in our lab (a radioisotope laboratory is necessary), an indirect method was developed for the determination of the dead time t_0 and the porosity ε of the clay/quartz columns used in our experiments. The investigated column is preconditioned by a constant flow of 40 µL min^{-1} with an eluent mixed with uncharged 1-bromopropane, and the signal intensity of ^{79}Br is recorded by ICP-MS (see also section 2.1.3). If the injection of 10 µL ultrapure water is repeated, each injection is detected by a negative signal of the ^{79}Br measurement curve. By evaluating the minima of these negative signals, the dead time can then be calculated by the difference between two negative signals with the corresponding time of injection as exemplary shown in Fig. 7.

Additionally, the dead volume or the dead time of the entire system (void time) from HPLC autosampler up to detection in ICP-MS including various columns and stationary phases (dwell time) used in the work were determined. By injecting 10 µL ultrapure water into an eluent stream of V= 40 µL min^{-1} ultrapure water with an addition of 20 µL L^{-1} 1-bromopropane, the dead time t_0, dead volume V_{dead} and porosity ε of the column types used were defined.

The obtained dead times and porosity values are shown in Table 5. The Union ZDV contains no stationary phase and a negligibly small geometric internal volume. Therefore no liquid-filled internal volume and thus no porosity of the column filling ε can be determined for this column type. The dead time t_0 of the Union ZDV (t_0=71.1 ± 0.5 s) corresponds to the dead time of the entire HPLC instrument from the injector to the nebulizer without column (void time). By multiplication with the eluent flow (40 µL min^{-1} corresponds to 0.667 µL s^{-1}) the corresponding dead volume V_{dead} of the instrument without column (void volume) is obtained to be 47.4 µL. The porosity ε is calculated here as the quotient of the liquid-filled inner volume of the respective column V_{liquid}, in each case after deduction of the void volume, and the calculated geometric column internal volume V_{geo} of the empty columns (L_c = 20 mm) as shown in section.

In a next step, dynamic retention experiments of Eu(III) as chemical analogon for trivalent actinids and other repository-relevant elements were carried out with the developed and validated MCE-ICP-MS coupling method. Further, important influencing variables on retention in claystone will be investigated.

3.2.6. MCE of Eu(III) in the presence of iodide as retention marker

When injecting small volumes via mini-column discrete peaks are expected as a measurement signal at the column outlet. When Eu(III) is injected once together with sodium iodide as injection marker (m(Eu(III)) = 90 ng; m(I^-) = 12 ng; V_{inj} = 2 µL) via a pure kaolinite column with m(kaolinite) = 200 mg, results show that even after a long waiting time (about 90 min) from the injection, no Eu(III) is eluted from the column (see Fig. 8). In contrast, the injection marker iodide shows a

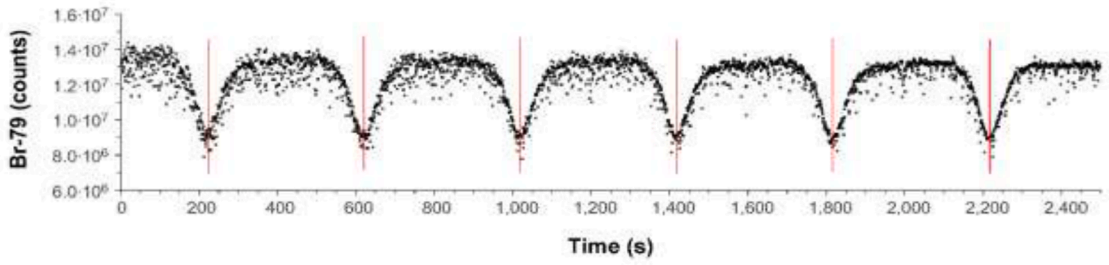

Fig. 7. Determination of the flow time (dwell time) by repeated injection of 10 µL ultrapure water into an eluent stream containing 1-bromopropane (10 µL 1-bromopropane in 500 mL ultrapure water) over a mini-column with 3.5 mm internal diameter and 285 mg column filling consisting of 1 wt.% OPA and 99 wt.% quartz sand (HPLC-ICP-MS coupling, flow 40 µL min^{-1}), and ICP-MS registration of the ^{79}Br signal.

Table 5
Dead times, volumes and porosity of the different column types used. Injection of 10 µL ultrapure water into an eluent stream of ultrapure water (V= 40 µL min^{-1}) with an addition of 1-bromopropane (20 µL L^{-1}); column length L_c = 20 mm.

Column	Filling	Mass (mg)	t_0 (s)	V_{dead} (µL)	V_{liquid} (µL)	V_{geo} (µL)	ε
Union ZDV	–	–	71.1 ± 0.5	47.4 ± 0.3	–	–	–
3.5 mm I.D.	SiO_2	293	211.1 ± 0.7	140.7 ± 0.5	86.7 ± 0.7	192	0.485
3.5 mm I.D.	1 wt.% OPA	285	224.0 ± 1.0	149.3 ± 0.7	140.7 ± 0.5	192	0.530

breakthrough after 270 s. Even with further injections of the same duration after the injection as well as with faster consecutive and numerous injections, no Eu(III) is initially eluted. Therefore, Eu(III) can be assumed to be quantitatively sorbed and completely retained by kaolinite.

Consequently, in the subsequent retention experiments with natural OPA, which as a clay mixture has a significantly higher cation exchange capacity (CEC = 105 meq kg^{-1}) [37] than the single mineral kaolinite (CEC = 9.4 meq kg^{-1}) [38], as column filling only 1 wt.% OPA was mixed with 99% quartz sand. In preliminary experiments, clear interactions with the injected Eu(III) could already be observed in this column filling material consisting of only about 3 mg clay beside the quartz (Fig. 6).

When repeatedly injecting 5 µl of a 2 mM europium perchlorate solution over a 1 wt.% OPA column (see Fig. 9), no europium signal can initially be detected for 20 injections. Only after the 21st injection Eu (III) is detectable at the column outlet. The measured signal increases from injection to injection (in total 13 injections) and remains at about the same level for the last five injections. The ^{24}Mg signal (that comes from the OPA) only serves to mark injections that have taken place recognisable, as no dedicated injection marker has been used at this stage of the experiments. It is noticeable that the ^{24}Mg signal initially decreases gradually as the number of injections increases, and more strongly with the breakthrough of Eu(III) as clearly seen in Fig. 9. A wash-out of the 1 wt.% OPA column material or a displacement of Mg from sorption sites of the clay material is assumed. Consequently, the injected Eu(III) first sorb quantitatively on the column. In the area of the signal increase only a fraction of the injected Eu(III), which decreases from injection to injection, remains on the column. Either no further Eu (III) is sorbed at the column and the injected quantity passes the column without delay in the saturation region. On the other hand, the injected Eu(III) is sorbed in the sense of a dynamic equilibrium and again displaces the same amount of Eu(III) from the column. With the experimental data currently available, it is not possible to distinguish between these two possibilities. In future experiments, injection of chemically similar terbium or, better, non-naturally occurring europium isotopes via a mini-column provided more information. In the subsequent detection step, the fate of the injected radioisotope on the column or the (unhindered) passage might be detected.

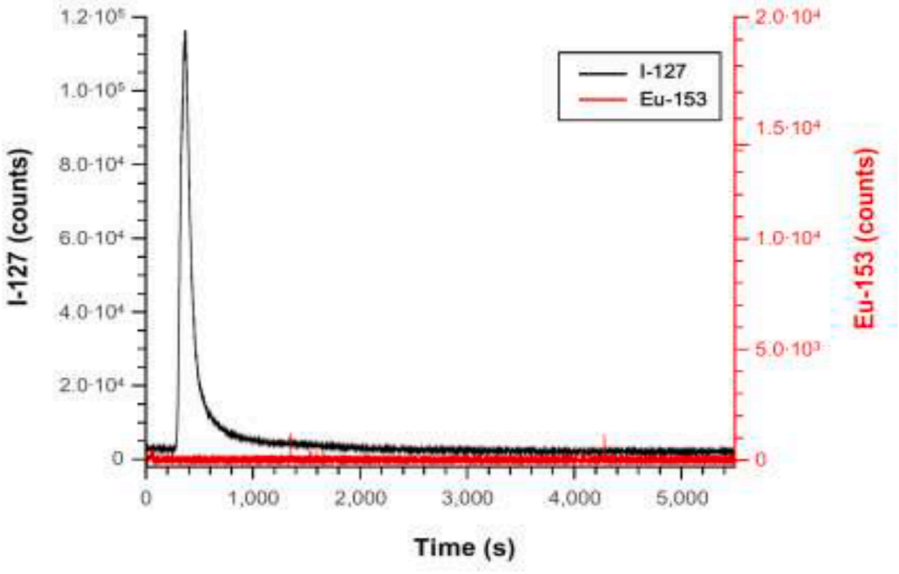

Fig. 8. Single injection of 90 ng Eu(III) together with 12 ng iodide dissolved in 2 µL ultrapure water (corresponds to 45 ppm Eu(III) and 6 ppm iodide) over a pure kaolinite column ($m_{kaolinite}$ = 200 mg) at a flow rate of 40 µL min^{-1} ultrapure water.

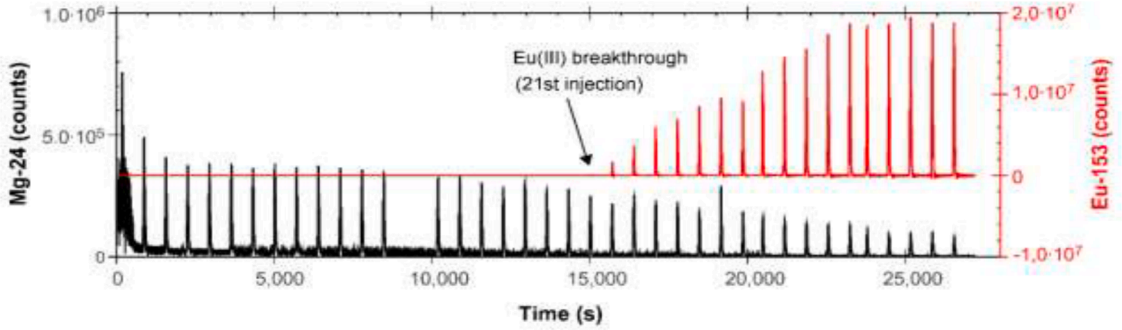

Fig. 9. Repeated injection of 5 µl each of a 2 mM europium perchlorate solution over a 1 wt.% OPA column. The breakthrough of the europium (upper measurement signal) occurred with the 21st injection. The ^{24}Mg trace (lower measurement signal) leached from the OPA in the column serves as a substitute for the injection marker not yet used in this experiment.

A rough estimate of the sorption capacity of the OPA in the column based on the cation exchange capacity (*CEC*) 10.5–12 meq 100 g^{-1} known from the literature [37,39] can be made by using the data from the experiment (m(column filling) = 293 mg; OPA content = 1 wt.%; m (OPA in column) = 1% 293 mg = 2.93 mg). Using this mass of the OPA contained in the column, it is now possible to calculate the sorption capacity for trivalent Eu(III):

$$\begin{aligned} \textit{Capacity}\ (Eu(III)) &= \frac{CEC}{3}\cdot M(Eu)\cdot m(OPA_{column}) \\ &= \frac{12\ meq/100\ g}{3}\cdot 152\frac{g}{mol}\cdot 2.93\ mg\ = 17.8\ \mu g \end{aligned} \quad (4)$$

With an injection volume V_{inj} of 5 mL at a Eu(III) concentration c(Eu) of 2 mM the mass of Eu(III) given up per injection m (Eu_{inj}) can be achieved:

$$m(Eu_{inj}) = V_{inj}\cdot c(Eu)\cdot M(Eu) = 5\mu L\cdot 2\ mM\cdot 152\frac{g}{mol} = 1.52\ \mu g \quad (5)$$

Dividing the sorption capacity of the column for trivalent Eu(III) by the mass of Eu(III) added per injection m (Eu_{inj}) gives the number of injections to saturation of the column $n_{inj,sat}$.

$$n_{inj,sat} = \frac{Capacity\ (Eu(III))}{m\ (Eu_{inj})} = \frac{17.8}{1.52} = 11.7\ \sim\ 12 \quad (6)$$

Based on the cation exchange capacity, the breakthrough should therefore occur after the twelfth injection of a 2 mM europium perchlorate solution. In the experimental (see text above and Fig. 9), the breakthrough of the Eu(III) only occurs with the 21st injection. As a result, the estimation based only on the *CEC* is insufficient. The above estimate neglects other sorption effects that are not based only on the exchange of cations of the clay and retention by precipitation. Especially on homogenised clay with its large surface area, surface complexation at corners and edges of the clay are also to be expected as shown for Eu(III) sorption on Ca-montmorillonite and Na-illite [40], which do not result only in an exchange of cations. In addition, any adsorption on the column wall and the quartz sand used for dilution is not considered. These effects would have to be additionally quantified and taken into account for a better estimation in the next experiments.

4. Conclusion and outlook

In a previous study, miniaturized clay column experiments using liquid chromatography were introduced to dynamically analyse sorption and desorption processes of UV active molecules on compacted clay. The focus of this work is the further development of such mini column experiments (column dimensions of 20 mm L x 3.5 mm I.D.) as a link between long-term diffusion experiments with experimental periods of several years in some cases, and batch experiments with unrealistic clay suspensions.

Through the current coupling with ICP-MS as a highly sensitive detector, MCE can now be performed as an injection-based online method. In the optimized setup, the standard ICP-MS configuration (Scott spray chamber and MicroMist nebulizer) was replaced by a PFA MicroFlow nebulizer with a flow range of only 40 µL min^{-1} (compared to the standard flow rate of at least 400 µL min^{-1}) and a 20 mL PFA cyclone spray chamber. By using MCE, retention as well as breakthrough experiments of ions such as iodide or even Eu(III) as a trivalent cation can be carried out on near-natural compact column filling materials in combination with realistic groundwater solutions without further additives in only a few minutes. Hereby, MCE-ICP-MS coupling allows clear measurement results to be obtained from dynamic metal sorption and desorption experiments under geochemical conditions close to nature. For our experiments, this means that no complexing ligands were used in the mobile phase and no synthetically produced stationary phase was used to separate the analytes.

First, the MCE were used only with ultrapure water and the clay mineral kaolinite. As a result, analytical parameters for characterizing the MCE were successfully derived. In a next step, Opalinus Clay (OPA) was used as a natural model clay mixture. To enable coupling with ICP-MS, the clay column was diluted with quartz sand thus revealing two important experimental aspects: Firstly, the swelling of pure OPA in contact with water leads to clogging of the column. Secondly, the enormous sorption capacity of OPA (more than ten times higher than kaolinite) made dilutions of OPA stationary phase necessary.

Injections of Eu(III) over a mini column of only 1 wt.% OPA (and 99 wt.% quartz sand) initially demonstrated that the entire injected amount of Eu(III) is sorbed. In addition, coupling with ICP-MS indicated that no Eu(III) was detected at the column outlet. For the first time, MCE results show that there is a high sorption capacity for trivalent cations, such as Eu(III), on compacted clay under near natural geochemical conditions. During the breakthrough phase, the eluted amount of europium increases with each further injection until the saturation phase (plateau of peak heights) is reached, in which no further increase in the eluted amount of europium is recorded.

In the next phase of development, MCE-ICP-MS will also be carried out in the presence of a highly saline eluent to simulate geochemical conditions for HLW disposals, such as those that occur in northern Germany. Additional coupling of MCE to triple quadrupole ICP-QQQ allows to detect also other relevant elements such as silicon at trace concentrations. Thus for example, MCE could help to identify important geochemical parameters that are relevant for the assessment of the retention behaviour for the long-term safety assessment of a future repository site in claystone as a potential host rock.

CRediT authorship contribution statement

Ralf Kautenburger: Supervision, Funding acquisition, Conceptualization, Methodology, Visualization, Writing – original draft. **Kristina**

Brix: Writing – review & editing, Validation, Visualization. **Sandra Baur:** Writing – review & editing, Validation, Visualization. **Jonas Michael Sander:** Investigation, Conceptualization, Methodology, Formal analysis, Visualization.

Declaration of Competing Interest

The authors declare that they have no known competing financial interests or personal relationships that could have appeared to influence the work reported in this paper.

Acknowledgement

This work was supported by the German Federal Ministry of Economics and Energy (BMWi), represented by the Project Management Agency Karlsruhe (PTKA-WTE) [grant no. 02E10991, 02E11415D and 02E11860D], and we would like to thank our project partners for the kind collaboration.

Supplementary materials

Supplementary material associated with this article can be found, in the online version, at doi:10.1016/j.talo.2022.100111.

References

[1] K.-J. Roehlig, H. Geckeis, K. Mengel, Facts and Concepts Disposal of radioactive Waste, Chem. Unserer. Zeit. 46 (3) (2012) 140–149.
[2] J.R. Duffield, D.R. Williams, John Jeyes Lecture. The environmental chemistry of radioactive waste disposal, Chem. Soc. Rev. 15 (3) (1986) 291–307.
[3] R. Kautenburger, H.P. Beck, Waste disposal in clay formations: influence of humic acid on the migration of heavy-metal pollutants, Chem. Sus. Chem. 1 (4) (2008) 295–297.
[4] C. Joseph, L. Van Loon, A. Jakob, R. Steudtner, K. Schmeide, S. Sachs, G. Bernhard, Diffusion of U (VI) in Opalinus Clay: influence of temperature and humic acid, Geochim. Cosmochim. Acta 109 (2013) 74–89.
[5] C.A.J. Appelo, L.R. Van Loon, P. Wersin, Multicomponent diffusion of a suite of tracers (HTO, Cl, Br, I, Na, Sr, Cs) in a single sample of Opalinus Clay, Geochim. Cosmochim. Acta 74 (4) (2010) 1201–1219.
[6] C.D. Shackelford, Laboratory diffusion testing for waste disposal — A review, J. Contam. Hydrol. 7 (3) (1991) 177–217.
[7] A.W. Miller, Y. Wang, Radionuclide interaction with clays in dilute and heavily compacted systems: a critical review, Environ. Sci. Technol. 46 (4) (2012) 1981–1994.
[8] R. Kautenburger, Batch is bad? Leaching of Opalinus clay samples and ICP-MS determination of extracted elements, J. Anal. At. Spectrom 26 (10) (2011) 2089–2092.
[9] R. Kautenburger, K. Brix, C. Hein, Insights into the retention behaviour of europium(III) and uranium(VI) onto Opalinus Clay influenced by pore water composition, temperature, pH and organic compounds, Appl. Geochem. 109 (2019), 104404.
[10] T.-H. Wang, M.-H. Li, S.-P. Teng, Bridging the gap between batch and column experiments: a case study of Cs adsorption on granite, J. Hazard. Mater. 161 (1) (2009) 409–415.
[11] R. Hahn, C. Hein, J.M. Sander, R. Kautenburger, Complexation of europium and uranium with natural organic matter (NOM) in highly saline water matrices analysed by ultrafiltration and inductively coupled plasma mass spectrometry (ICP-MS), Appl. Geochem. 78 (2017) 241–249.
[12] C. Hein, J.M. Sander, R. Kautenburger, New approach of a transient ICP-MS measurement method for samples with high salinity, Talanta 164 (2017) 477–482.
[13] M.-H. Li, T.-H. Wang, S.-P. Teng, Experimental and numerical investigations of effect of column length on retardation factor determination: a case study of cesium transport in crushed granite, J. Hazard. Mater. 162 (1) (2009) 530–535.
[14] A.K. Das, R. Chakraborty, M.L. Cervera, M. de la Guardia, Metal speciation in solid matrices, Talanta 42 (8) (1995) 1007–1030.
[15] R. Kautenburger, A new timescale dimension for migration experiments in clay: proof of principle for the application of miniaturized clay column experiments (MCCE), J. Radioanal. Nucl. Chem. 300 (1) (2014) 255–262.
[16] Y. Yang, J.E. Saiers, N. Xu, S.G. Minasian, T. Tyliszczak, S.A. Kozimor, D.K. Shuh, M.O. Barnett, Impact of natural organic matter on uranium transport through saturated geologic materials: from molecular to column scale, Environ. Sci. Technol. 46 (11) (2012) 5931–5938.
[17] J. Lewis, J. Sjöstrom, Optimizing the experimental design of soil columns in saturated and unsaturated transport experiments, J. Contam. Hydrol. 115 (1–4) (2010) 1–13.
[18] M.A. Dangelmayr, P.W. Reimus, N.L. Wasserman, J.J. Punsal, R.H. Johnson, J. T. Clay, J.J. Stone, Laboratory column experiments and transport modeling to evaluate retardation of uranium in an aquifer downgradient of a uranium in-situ recovery site, Appl. Geochem. 80 (2017) 1–13.
[19] H. Liu, J. Randon, Behavior of micro pillar array column in high pressure gas chromatography, J. Chromatogr. A 1656 (2021), 462551.
[20] L. Labied, P. Rocchi, T. Doussineau, J. Randon, O. Tillement, F. Lux, A. Hagège, Taylor dispersion analysis coupled to inductively coupled plasma-mass spectrometry for ultrasmall nanoparticle size measurement: from drug product to biological media studies, Anal. Chem. 93 (3) (2021) 1254–1259.
[21] M. Thomas, Miniaturisierte Säulenversuche zur Untersuchung der Migration von Schadstoffen in Geologischen Matrizes, Naturwissenschaftlich-Technische Fakultät, Universität des Saarlandes, Saarbrücken, 2008.
[22] R. Michalski, Applications of Ion Chromatography for the Determination of Inorganic Cations, Crit. Rev. Anal. Chem. 39 (4) (2009) 230–250.
[23] J. Proch, P. Niedzielski, Iron species determination by high performance liquid chromatography with plasma based optical emission detectors: HPLC–MIP OES and HPLC–ICP OES, Talanta 231 (2021), 122403.
[24] A.A. Ammann, Speciation of heavy metals in environmental water by ion chromatography coupled to ICP–MS, Anal. Bioanal. Chem. 372 (3) (2002) 448–452.
[25] R. Michalski, M. Jabłonska, S. Szopa, A. Łyko, Application of Ion Chromatography with ICP-MS or MS detection to the determination of selected halides and metal/metalloids species, Crit. Rev. Anal. Chem. 41 (2) (2011) 133–150.
[26] M. Grotti, A. Terol, J.L. Todolí, Speciation analysis by small-bore HPLC coupled to ICP-MS, TrAC Trends Anal. Chem. 61 (2014) 92–106.
[27] C. Joseph, K. Schmeide, S. Sachs, V. Brendler, G. Geipel, G. Bernhard, Sorption of uranium(VI) onto Opalinus Clay in the absence and presence of humic acid in Opalinus Clay pore water, Chem. Geol. 284 (3–4) (2011) 240–250.
[28] Nagra, Projekt Opalinuston-Synthese der Geowissenschaftlichen Untersuchungsergebnisse, Entsorgungsnachweis für Abgebrannte Brennelemente, Verglaste Hochaktive Sowie Langlebige Mittelaktive Abfälle, Technischer Bericht /Nagra (NTB) 02-03, 2002. Nagra Wettingen, Switzerland.
[29] M. Lauber, B. Baeyens, M.H. Bradbury, Physico-chemical characterisation and sorption measurements of Cs, Sr, Ni, Eu, Th, Sn and Se on Opalinus Clay from Mont Terri, Paul Scherrer Inst (2000).
[30] V.R. Meyer, Praxis Der Hochleistungs-Flüssigchromatographie, John Wiley & Sons, 2009.
[31] C.M. Marquardt, Interaction and transport of actinides in natural clay rock with consideration of humic substances and clay organic compounds, KIT Sci. Rep. (2012) 7633.
[32] H.M. Rietveld, A profile refinement method for nuclear and magnetic structures, J. Appl. Crystallogr. 2 (2) (1969) 65–71.
[33] H. Freundlich, O. Schmidt, G. Lindau, Über die Thixotropie von Bentonit-Suspensionen, Kolloid-Beihefte 36 (1) (1932) 43–81.
[34] R.G. de Kretser, D.V. Boger, A structural model for the time-dependent recovery of mineral suspensions, Rheol. Acta 40 (6) (2001) 582–590.
[35] J. Klawiter, M. Kamiński, J.S. Kowalczyk, Investigation of the relationship between packing methods and efficiency of preparative columns: I. Characteristics of the tamping method for packing preparative columns, J. Chromatogr. A 243 (2) (1982) 207–224.
[36] S. Maestre, J. Mora, J.-L. Todolí, A. Canals, Evaluation of several commercially available spray chambers for use in inductively coupled plasma atomic emission spectrometry, J. Anal. At. Spectrom. 14 (1) (1999) 61–67.
[37] R. Kautenburger, K. Brix, C. Hein, Insights into the retention behaviour of europium(III) and uranium(VI) onto Opalinus Clay influenced by pore water composition, temperature, pH and organic compounds, Appl. Geochem. 109 (2019).
[38] R. Kautenburger, H.P. Beck, Influence of geochemical parameters on the sorption and desorption behaviour of europium and gadolinium onto kaolinite, J. Environ. Monitor. 12 (6) (2010) 1295–1301.
[39] M. Klinkenberg, R. Dohrmann, S. Siegesmund, Laboratory Testing of Opalinus Clay (LT) Experiment: Comparison of Opalinus Clay and Callovo-Oxfordian Clay-Stone With Respect to Mechanical Strength and Carbonate Microfabric, 2008.
[40] M. Bradbury, B. Baeyens, H. Geckeis, T. Rabung, Sorption of Eu (III)/Cm (III) on Ca-montmorillonite and Na-illite. Part 2: surface complexation modelling, Geochim. Cosmochim. Acta 69 (23) (2005) 5403–5412.